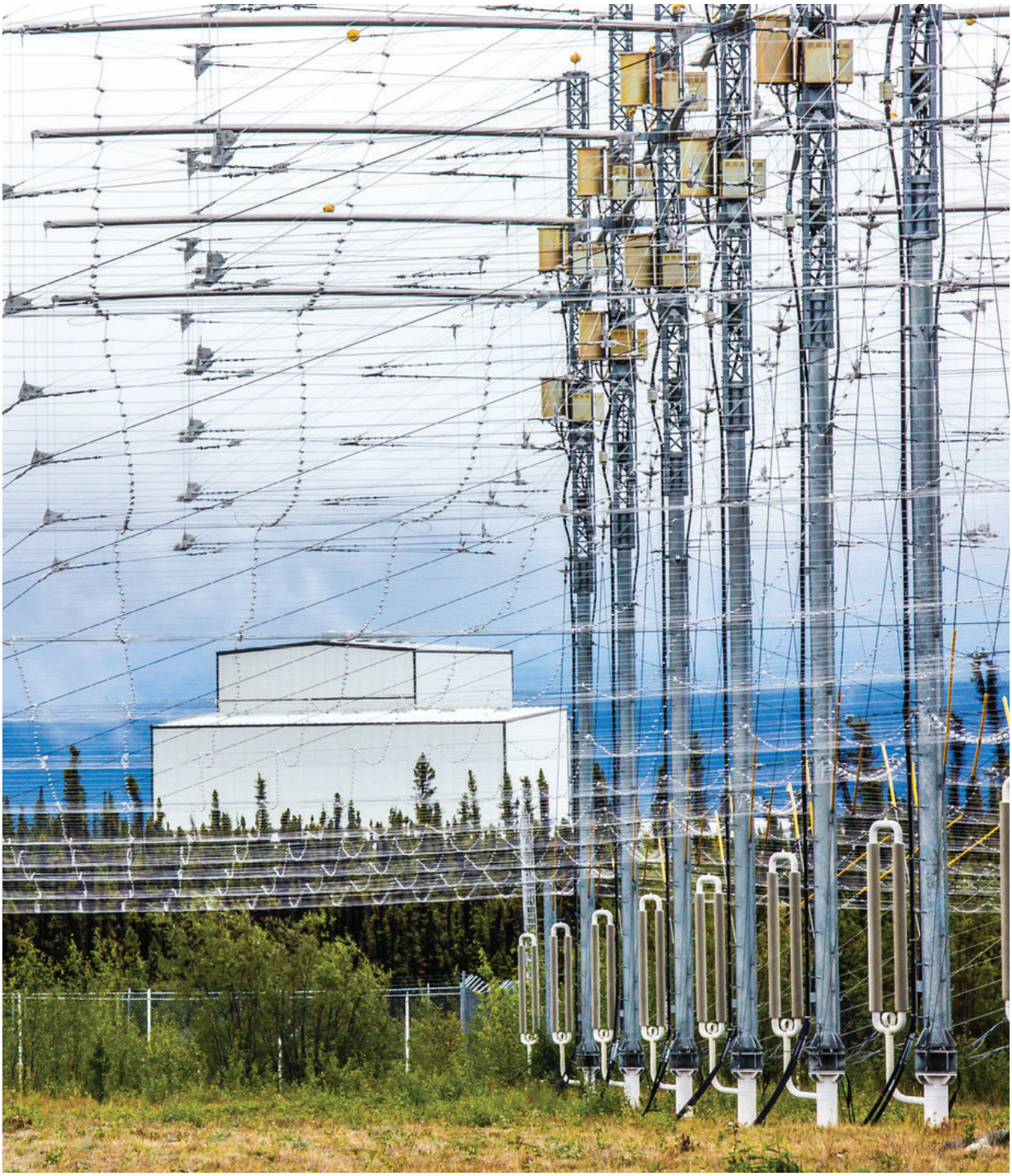

The case for

ESTABLISHING A SPACE PHYSICS AND RADIO SCIENCE OBSERVATORY

at Gakona, Alaska

The case for

ESTABLISHING A SPACE PHYSICS AND RADIO SCIENCE OBSERVATORY

at Gakona, Alaska

This report describes the existing High Frequency Active Auroral Research Program (HAARP) facilities and the vision for applying them. It makes a case for establishing the observatory by describing the unique and highly valuable new research it will enable. The HAARP facilities, located in Gakona, Alaska, were operated by the Air Force Research Laboratory (AFRL) from 1993 until 2014. The facilities consist of a large high-power (3.6 MW) high-frequency radio transmitter and associated diagnostic instruments used for ionospheric modification experiments. After discontinuing the HAARP program, the Air Force donated the HAARP equipment to the University of Alaska Fairbanks (UAF). Now in possession of these world-leading facilities, UAF is working toward establishing an observatory centered on their unique capabilities. The observatory will focus on RF ionospheric heating, Radio Science, Aeronomy, and Magnetospheric Physics. It will bring together a broad range of instrumentation to function as a year-round observatory. By applying ionospheric modification to the problems of Aeronomy and Magnetospheric Physics, the controlled experimentation techniques of laboratory science will be brought to bear on study of the natural near-earth space environment.

Gakona is located in south central Alaska at 62°23' (63.44° magnetic) North Latitude and 145°09' West Longitude, about 2.5° south of Fairbanks, which places it in the sub-auroral region most of the time. The location has proven to be fruitful for ionospheric modification studies of the generation of ELF and VLF radio emissions by modulating the auroral electrojet, and for studies of the injection of these waves into the magnetosphere to observe their interaction with radiation-belt energetic particles. The subauroral region is relatively under sampled as compared to the auroral zone and lower latitudes. It is however becoming recognized as playing a critical role in many aspects of magnetospheric dynamics. Establishing an observatory in this region at a location in close proximity to all of the auroral zone instruments in Alaska will enable ground-breaking new research. It will enable addressing such questions as:

- What is the relationship between electron precipitation and proton precipitation with respect to substorm onsets?
- Are Extremely Low Frequency (ELF) and Very Low Frequency (VLF) radio emissions a significant factor in the precipitation of energetic particles from the radiation belts?
- What is the neutral atmospheric density profile in the lower thermosphere and how does it vary on time scales of minutes to days?
- How does the profile of neutral winds in the lower thermosphere evolve with time?
- What are the charge states of the meteoric dust particles in polar mesospheric clouds?
- What is the mechanism for generation of hiss and chorus waves in the magnetosphere?
- To what extent do cold-plasma ducts guide VLF radio emissions into the magnetosphere?

The list of topics that can be addressed at the site is extensive and spans Aeronomy, Magnetospheric Physics, Radio Science, and (obviously) the physics of the interaction of electromagnetic waves with plasmas. This report describes a number of these topics and how we envision an observatory at Gakona can contribute to advancing our knowledge in each area. It is not a litany of previous results, but rather it focuses on new research that can be expected.

2. Gakona in Geospace

As illustrated in Figure 1, HAARP is located just equatorward of L=5. While this location is referred to as subauroral, because the auroral oval is offset from the magnetic pole by several degrees of latitude in the anti-sunward direction, Gakona's location relative to the oval changes substantially throughout the day. Around noon, Gakona is well equatorward of the auroral oval and auroral effects are rare, even during geomagnetically active times. At dawn and dusk, Gakona is typically within a few degrees of the equatorward edge of the auroral oval. During active periods, both auroral currents and auroral precipitation may be present above Gakona. At midnight, Gakona is at the edge of the auroral oval, and during active times is an ideal location to observe the development of auroral phenomena as the oval expands equatorward, especially when combined with observations from farther north.

The observatory at Gakona, if suitably equipped, would be a uniquely capable multi-instrumented facility (CEDAR Class 1 facility) centered at sub-auroral latitude with great discovery class science potential. Canada has many sites with magnetometers, optical instruments, ionosondes, and other small instruments at latitudes below the auroral zone, but none offer a full complement of geoscience observing instruments. The central sub-auroral location of Gakona means that multi-instrument coordinated observations of important processes in both the neutral and ionized atmosphere can be conducted directly within the sub-auroral D and E region ionosphere in a way not possible with other ISR facilities. In this era of modern, multi-scale science, there is a compelling need for intense study of the sub-auroral ionosphere, especially as the region is rich with unique phenomena, many of which are not well understood. Recent studies based on both ground-based and space-based observations suggest subauroral phenomena are closely linked to those occurring at higher latitudes--all manifestations of system-like coupling between the ionosphere, thermosphere, and magnetosphere. The lack of comprehensive measurements at latitudes equatorward of the auroral oval is a barrier to full understanding of the entire space weather system.

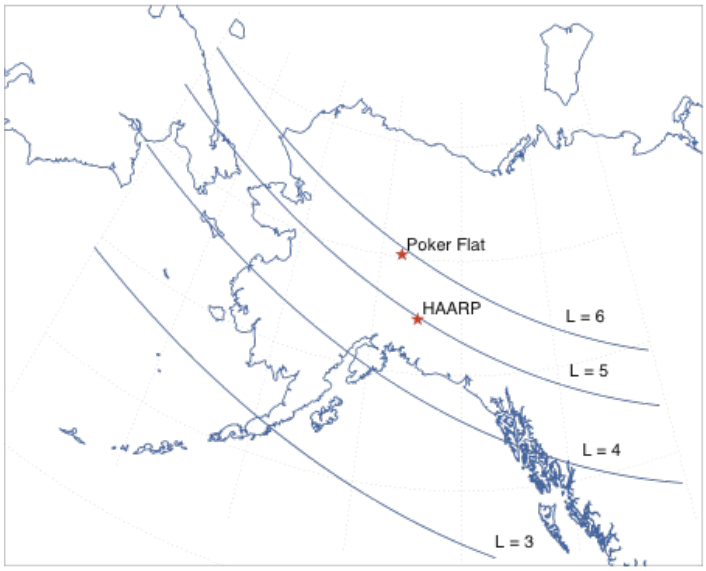

Figure 1. Location of HAARP and Poker Flat with L-shell contours over the Alaska region

The list of phenomena to be studied by an observatory in the sub-auroral region should include: Diffuse Aurora, Proton Aurora, Pulsating Aurora, Omega Bands, Westward Traveling Surges, Type A Red Aurora, SAR Arcs, Ring Current Aurora, Detached Arcs, Ionospheric Trough, Sub-Auroral Ion Drifts (SAID), Sub-Auroral Polarization Streams (SAPS), among others.

As an example of subauroral observations, Figure 2 shows a meridional cross section of ionospheric electron densities measured by the Chatanika radar. A simultaneous overpass of the NOAA-6 satellite showed that

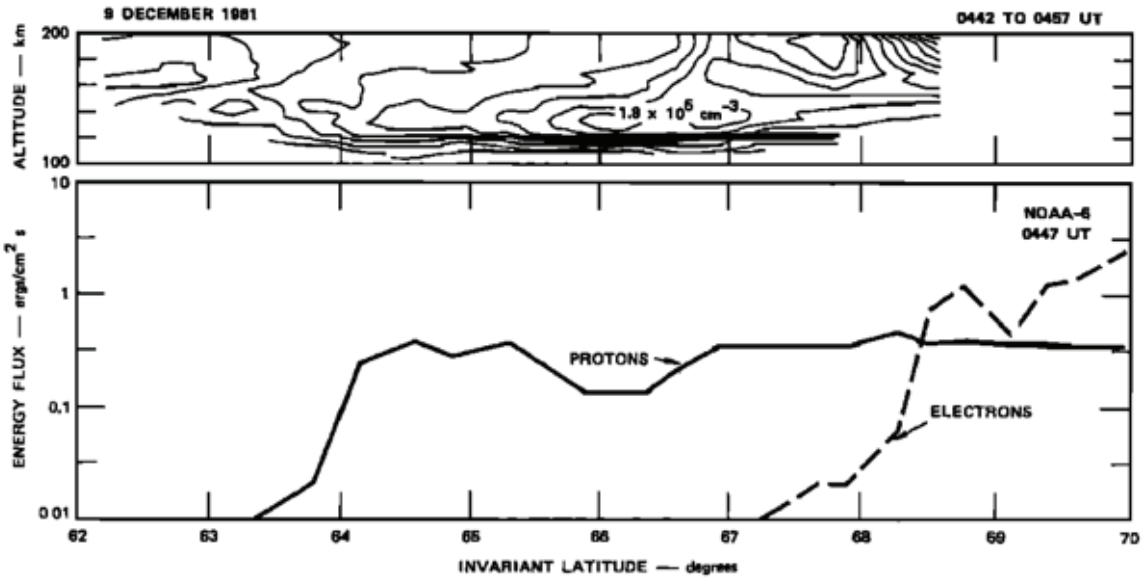

Figure 2. Incoherent-Scatter radar observations of electron densities (upper), and satellite based observations of energetic precipitation (lower) from 9 December 1981.

the entire E- region ionosphere from 63° to 67° latitude was produced by a broad region of precipitating protons.

Many magnetospheric processes taking place at the onset of substorms are observed at the equatorward edge of the auroral oval. At a magnetic latitude of 63°, an observatory at Gakona would be well situated to provide important diagnostic information about these phenomena.

3. Observatory vision

While the existing list of instrumentation in the state of Alaska is extensive, augmenting the complement at Gakona would greatly enhance our ability to research fundamental questions of space physics and aeronomy. Figure 3 shows the array of instrumentation in Alaska as of July 2016. Superposed over the map is a composite image formed from a number of passes of the Special Sensor Ultraviolet Spectrographic Imager (SSUSI) on the Defense Metorological Satelite Program (DMSP) satellites. The figure demonstrates that Poker Flat and the observatories to the north span the high-latitude portion of the auroral oval and (often) into the region of open field lines. An observatory at Gakona would extend the coverage to the subauroral region and inner magnetosphere.

Instrumentation already present at Gakona includes an all-sky imager from the Themis ground-based observatory (GBO), a UAF digital all-sky imager, narrow-field imagers, GPS TEC and scintillation receivers, a fluxgate magnetometer, and a DPS-4D Digisonde. We envision adding filtered digital all-sky

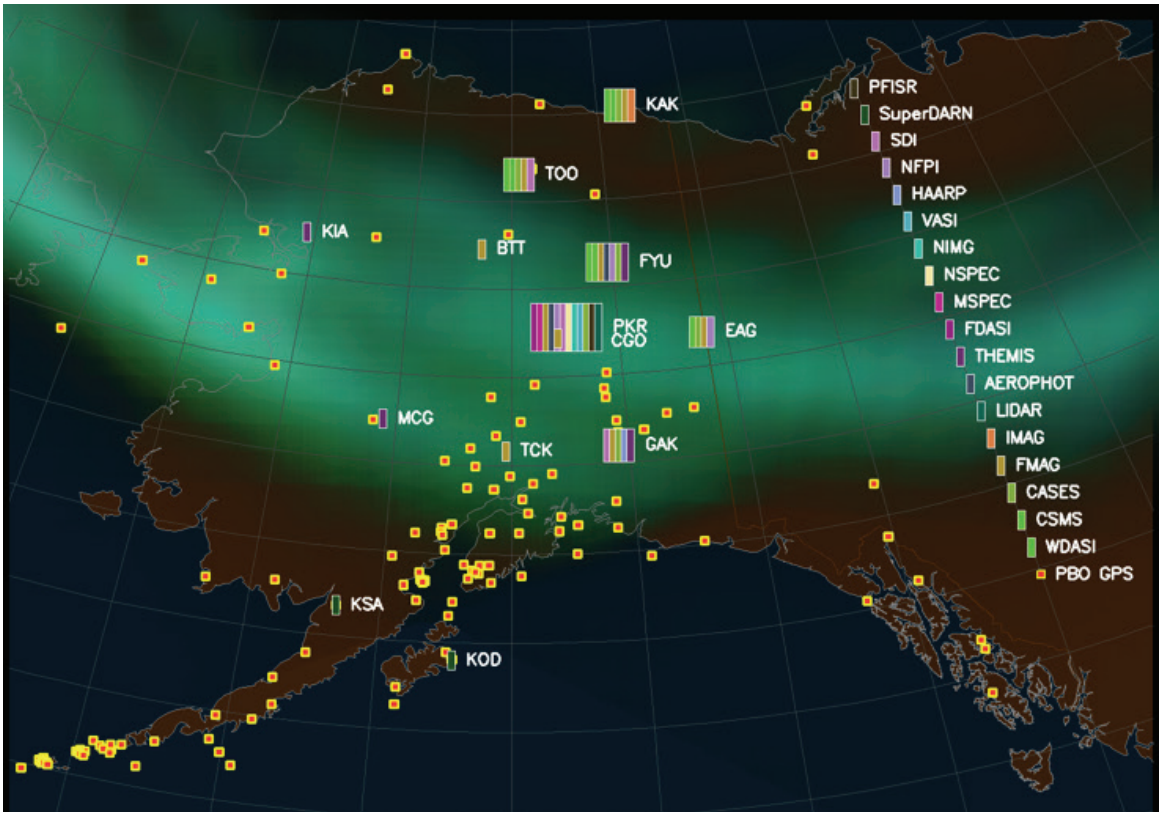

Figure 3. Space-observing instrumentation in Alaska

imager, a meridian spectrograph, a near-IR all-sky camera, and a narrow-field Fabry-Perot interferometer. Instrumentation from experimenters outside of UAF is welcome at the site and a number of researchers are already taking steps to deploy their systems.

The center-piece of instrumentation at the site would be an incoherent-scatter radar (ISR). The synergy between ISR observation and RF Ionospheric modification is significant as is demonstrated in research at EISCAT and the past work at Arecibo. Despite the fact that HAARP is a much more capable facility than the EISCAT heater at Tromsø, the scientific program at Tromsø has flourished with the collocation of an incoherent scatter radar (ISR) whereas the program at HAARP has been held back for lack of one. (EISCAT reports an average of 38 heater related publications per year.) Ionospheric heating modifies the state parameters of the ionosphere, notably the electron temperature and density, and an ISR is the most capable tool we have for quantifying heating effects from the ground. An ISR at HAARP would permit investigators for the first time to measure D–region temperature profiles, assess the absorption of the HF pump waves, and gauge the efficiency of every heating experiment. Quantifying absorption by other means is usually impractical. Unquantified absorption makes it difficult to know how well any experiment at HAARP is performing and in some cases, such as experiments to determine threshold electric fields, it is impossible to obtain accurate results. The ISR technique would also permit the measurement of density profile changes caused by heating. Without such measurements, it is difficult to know whether the changes are caused by thermodynamic or chemical effects or by ionization due to electron acceleration.

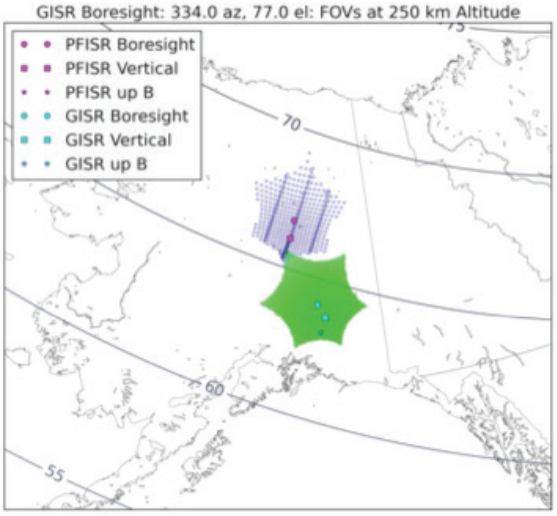

Figure 4. F-region fields-of-view for PFISR and GISR

Heating experiments also create electrostatic waves, notably enhanced ion-acoustic and Langmuir waves, which can be directly observed by ISRs. These observations are essential for studying Langmuir turbulence and associated nonthermal effects. An ISR furthermore gives a synoptic view of heating experiments and can reveal unexpected results such as unanticipatedheating effects from X-mode emissions observed recently at EISCAT. Discovery and especially closure in most every avenue of heating research require a collocated ISR.

All areas of research at the site would be enhanced by the addition of an ISR. And, having two ISRs in Alaska within a few hundred kilometers of each other creates an observing geometry that has never existed. The configuration would enable research on a number of exciting topics, providing observations that could not be obtained otherwise. Figure 4 shows fields-of-view (FOV) for one potential configuration of the existing Poker Flat ISR (PFISR) and a new Gakona ISR (GISR). The figure shows the FOV for F-region observations and illustrates a small region of common volume observations. Even this small region of overlap between the fields of view is significant in that it constrains solutions for the velocity field over the full extended-region of observations, and removes the inherent ambiguity from fits to line-of-site observations from a single site. The reason for this is that the divergence of the velocity perpendicular to the magnetic field has to be zero everywhere (incompressible magnetic field). Having line-of-site observations from two directions provides enough information to determine true vectors in the overlap region, and uniquely determines the divergence through the remainder of the region of observations.

An abbreviated list of research topics enabled by such an ISR configuration includes:

- D- and E-region neutral wind estimates at two points separated by 330 km. Cross-correlation to obtain wavelengths, distinguish tidal modes and planetary waves, monitor equatorward motion of pulses launched by aurora.
- Statistics and case studies of D-region radiation belt precipitation at two different L-shells
- Statistics and case studies of PMSE at two different latitudes.
- F-region density and temperature imaging over the union of the two FOVs.
- Vector electric field estimation over the union of the two FOVs.
- Unambiguous derivation of ion upflow velocity in more directions than just up-B
- Ion temperature anisotropy measurements
- Away from perpendicular thermal scatter experiments in a common volume with parallel Naturally Enhanced Ion Acoustic Line (NEIALs) measurements.
- Bistatic ISR spectrum to probe smaller Bragg wavenumber (larger scales)
- Larger scales -> Narrower ISR spectra
- Larger scales -> smaller finite Debye length corrections -> allows for absolute determination of Te

4. Education and Outreach
HAARP has a unique role to play in student education. For many years HAARP hosted a summer school known as Polar Aeronomy and Radio Science (PARS). PARS typically drew about twenty to twenty five students from a broad spectrum of US universities, mostly graduate students but some undergraduates. The 10-day summer school included several days of scientific talks and tutorials, and several days at the HAARP facility.

Each student in attendance devised and carried out his or her own experiment and was given at least a few hours of time during the experimental days. Usually, one of several instruments in the field was used, its data analyzed and presented by the student at the end of the school.

Figure 5. Photo of the PARS group from the 2003 school

Although a number of summer schools exist in geospace topics, PARS is unique in allowing students to actively carry out an experiment, from beginning to end. Essentially, PARS takes students through the entire scientific process: scholarly background, experimental design and execution, and analysis, and presentation of results. Although the results presented at the school were often fairly rough and preliminary, further analysis of PARS experiments directly led to numerous papers in major journals, and contributed to many PhD dissertations.

5. Heating Theory
As the worlds most powerful and flexible ionospheric heater, HAARP is able to push the envelope of RF plasma heating theory. It can produce an effective radiated power that is a factor of two higher than the EISCAT facility, the second most powerful, and can do so over its full frequency range rather than at the limited frequencies available to other facilities. It was designed with this power to enable investigation of non-linear effects in the plasma; effects that can not be investigated at the other heating facilities. The following paragraphs list some open questions of ionospheric heating and how HAARP can contribute toward their solution.

Is heating creating ionization? (requires ISR) Enhanced optical airglow was one of the first phenomena associated with ionospheric modifications by high power HF waves [Biondi et al., 1970; Haslett and Megill,

1974; Adeishvili et al., 1978] and continues to be the focus of research (see review by Gurevich [2007]). While it was first thought that the enhancements could be explained by heating and the widening of the tail of the thermal electron population [Mantas , 1994; Mantas and Carlson , 1996], the measured ratios of red- and green-line emissions and the presence of optical emissions with high energy thresholds signaled a non-thermal component of the electron energy distribution [Bernhardt et al., 1989; Gustavsson et al., 2001a, 2003; Djuth et al., 2005; Gustavsson et al., 2005]). Observations of the O+ 732–733 nm emission consistent with electron impact ionization also supported this proposition [Mutiso et al., 2008].

More recently, Pedersen et al. [2010] reported the creation of a layer of ionization over HAARP sufficiently dense to support additional ionospheric interactions. The layer (as seen in ionograms) was produced initially at 220 km altitude using full power O-mode HF heating in the direction of magnetic zenith and at a pump frequency very close to the second electron gyroharmonic frequency at that altitude. Once produced, the layer descended to a terminal altitude of about 150 km. Layer production was accompanied by intense optical emissions, which were filamentary and highly intermittent spatially.

The proposition of artificial ionization through ionospheric heating is also supported by other measurements. Rose et al. [1985] published in situ measurements from rocket experiments showing electron energies up to 10 eV. Carlson et al. [1982] published incoherent scatter plasma line measurements establishing suprathermal electron spectra reaching at least 20 eV. Estimates of the suprathermal electron energy tail on the basis of airglow measurements at multiple emission lines (e.g. 630.0, 557.7, 777.4, 844.6, and 427.8 nm) have been formulated by Bernhardt et al. [1989]; Gustavsson and Eliasson [2008]; Hysell et al. [2012, 2014b].

The only compelling evidence for artificial ionization layers comes from HAARP. Given the absence of a collocated ISR, these results must be regarded tentatively, as the actual amount of ionization created is still under debate. The ability to create energetic electron populations and artificial ionization is compelling since it could allow laboratory-grade experiments on the processes involved in the natural aurora. More investigation with better diagnostics is necessary.

Is the standard model of heating accurate and complete? The standard model in particle physics predicts all of the subatomic particles that are thought to be consistent with the interactions allowed between matter. Feynman diagrams are a graphical description of those interactions. The recent history of high-energy physics has been consumed with finding all of the particles (quarks, leptons, gauge bosons, Higgs boson) in the laboratory.

Something similar has been occurring in the field of ionospheric modification. The Manley-Rowe equations reflect the conservation of energy and momentum in wave-wave interactions and govern the waves that can be created in heating experiments. For example, in the parametric decay instability, the pump EM wave decays into two electrostatic waves – an ion acoustic wave and a Langmuir wave. The interaction can be described graphically by the triad of the three wavevectors in something resembling a Feynman diagram.

The Langmuir wave can then undergo further decay into another Langmuir and ion acoustic wave, the former being slightly shifted in frequency. A cascade process can thus ensue until the pump-wave energy

falls below threshold for instability. Finally, the Langmuir waves can produce electromagnetic waves through linear mode conversion (in the presence of density irregularities) that can propagate to the ground and be detected with radio receivers as stimulated electromagnetic emission (SEE).

Other auxiliary electrostatic waves can be involved in the three- and four-wave interactions are upper-hybrid and lower-hybrid waves, and purely growing (zero-frequency) modes. The SEE spectrum finally observed contains a number of broad and narrow line features indicative of the various allowed interactions and cascades.

Almost every allowed interaction has been observed in SEE experiments. There are two notable exceptions – the two-plasma decay instability and the stimulated Raman scatter instability. The ongoing search for these interactions is akin to the search for elementary particles in the particle physics standard model.

What power level is required to drive ionospheric plasma distributions out of Maxwellian range? Ordinarily, the distribution of particle velocities in any gas is well described by a Maxwellian distribution, which means that just one parameter, temperature, is sufficient to describe it. If a plasma is perturbed fast enough, however, it can acquire a velocity distribution that is non Maxwellian. We know that such perturbations can be caused by, for example, the powerful electromagnetic pulse from lightning or from a nuclear weapon. The question of the velocity distribution being Maxwellian or non-Maxwellian greatly affects the recovery time and electrical conductivity that our models would predict.

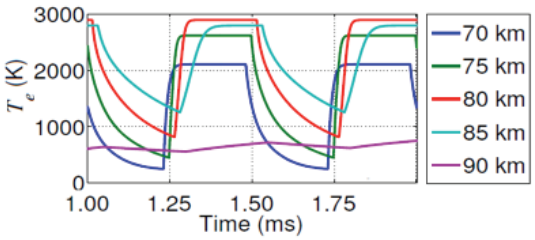

Figure 6. Simulated temperatures as a function of time during heating

As part of our efforts to understand how the ionosphere may respond to other external drivers (like solar flares and geomagnetic storms), it is important to quantify the level of disturbance required to drive the distribution away from Maxwellian, and to quantify the time for recovery after a disturbance. HAARP's incredibly high effective radiated power (ERP) enables experiments to do just that. Figure 6 shows a simulation of D-region electron temperatures during heating, which reach 3000 K as quickly as 10s of microseconds after the initiation of heating. This provides a unique opportunity to study how the ionosphere reacts to a rapid-onset disturbance, and to determine the threshold where non-Maxwellian physics becomes important. Since HAARP has easily the highest ERP of any HF heating facility in the world, it is the only facility capable of addressing this scientific question.

What ionospheric conditions lead to fine-scale heater-induced airglow structure? What mechanism causes this phenomenon and can it be related to fine-scale auroral processes? Optical emissions provide an invaluable remote sensing diagnostic of energy deposition in a plasma. Modern spectral imaging system can produce space-time maps of airglow and auroral processes at ~50-m spatial and ~10-ms temporal resolution. These scales are inaccessible to active remote sensing techniques such as incoherent scatter radar (ISR). Indeed our knowledge that geospace energy deposition processes cascade to such sub-gyroradius scales rests with

optical evidence. Decameter-scale structure has been observed in both natural aurora and heater-induced airglow. Neither is observed frequently and the ionospheric conditions appear to dictate whether or not the plasma will be driven to this state.

Imaging systems deployed to the HAARP facility have captured spectacular high-resolution video of heater-induced emissions (Figure 7 left). Small-scale rayed artificial airglow was observed on October 28,2008 at HAARP by the telescopic imager [Kendall et al., 2010]. This airglow occurred during an experiment at twilight from 2:55-4:00 UT (18:55-20:00 LT) and with estimated scale sizes of 100 m (at assumed 225 km altitude), constitutes the smallest known structure observed in artificial airglow. The airglow consisted of rays that appeared to be oriented along the geomagnetic field lines. The mechanism producing the observed filaments remains at present largely speculative. These displays have similarities to natural aurora observed during substorm dipolarization events (Figure 7 right). The filaments in this display are thought to be connected to breaking Alfven waves in the near-Earth magnetosphere [Dahlgren et al., 2013], but our understanding is far from complete. Although the details of energy transfer differ in these two cases, common modes must be at play. Both the natural and "artificial" cases involve wave-particle interactions, and both involve kinetic-scale physics. The collocation of HAARP, AMISR, and high-resolution optical sensors will provide an ideal laboratory for advancing our understanding of fine-scale structure in space plasmas.

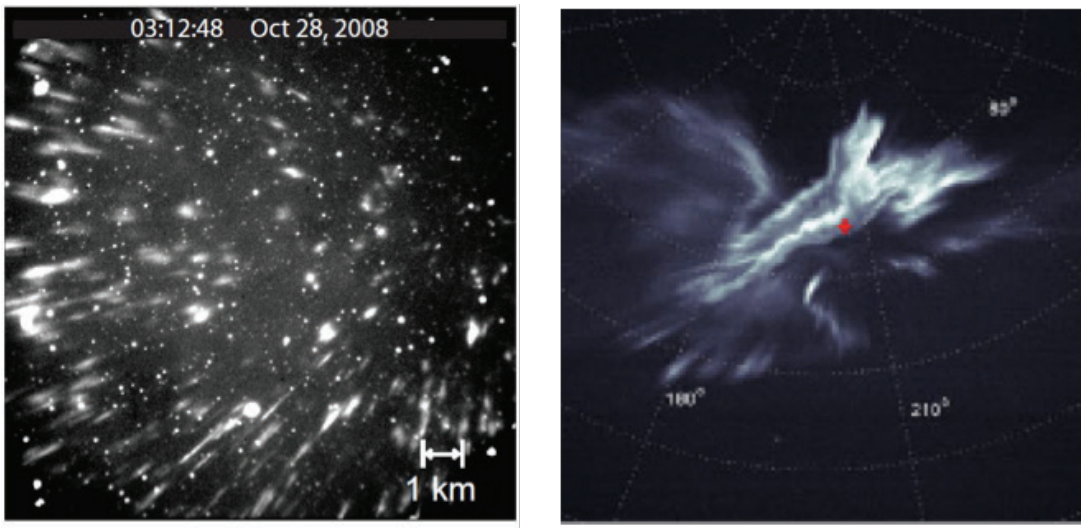

Figure 7. Left: Observations of airglow field produced during HAARP experiment (557.7 nm, 1-s exposure). Right: Aurora observed during substorm expansion phase (prompt emission filter, 20-ms exposure. Both images cover a 15x15 km field of view at 120 km altitude.

Is our scientific understanding of radio propagation through a heated ionosphere complete? Heating the ionosphere using the HAARP HF transmitter modifies the electron temperature of the D-region ionosphere and, in turn, changes the propagation characteristics of radio waves traversing the heated patch of ionosphere. Ionospheric cross-modulation, or the Luxembourg Effect, as this phenomenon has come to be known, has been used to probe the properties of the lower ionosphere for over 60 years [e.g., Fejer, 1955, 1970; Weisbrod et al., 1964; Senior et al., 2010; Langston and Moore, 2013]. Tellegen [1933] first

observed cross-modulation experimentally, and shortly thereafter, the basic physical processes describing cross-modulation were identified [e.g., see Huxley and Ratcliffe, 1949]. Recent measurements of the cross-modulated signal observed at HAARP and at EISCAT have been interpreted successfully using current ionospheric heating models and good assumptions about the properties of the lower ionosphere [Senior et al., 2010; Langston and Moore, 2013]. While Langston and Moore [2013] presented observations with the highest sample rate and signal-to-noise ratio, thanks to HAARP's high ERP and high quality transmission control, observations at EISCAT were further restricted using radar and ISR observations of the D-region electron density and temperature; it was determined that present models cannot accurately predict the observations, given the restrictions [Senior et al., 2010]. Cross-modulation experiments at HAARP would benefit tremendously from the simultaneous use of an ISR to quantify D-region properties and determine whether or not present models properly predict radio wave propagation through the modified ionospheric region.

6. Application to Aeronomy

The location of Gakona makes it ideal for studying many subauroral phenomena and their connection to magnetospheric processes. Some studies are enabled by the heating array, while others are enabled simply by virtue of the subauroral location. Among the various topics that can be investigated without the heater are proton precipitation, radiation belt precipitation, sub-auroral polarization streams (SAPS) and aurorally generated gravity waves.

Although it is well known that proton precipitation can be a significant contributor to diffuse aurora, particularly in the evening sector, questions remain about what magnetospheric processes are responsible for the variable fluxes. Burke et al. [2002] referred to proton aurora as detached proton arcs, as observed in space-based images, and were associated with ionospheric features that are the manifestation of plasma plumes in the plasmasphere [Spasojevic et al. 2004].

Because of their higher mass, protons represent a major indicator of magnetospheric plasma pressure. Gradients in plasma pressure in the magnetotail give rise to the Region 2 field-aligned currents. Thus, the proton aurora may be a signature of variability in the ring current, with which the Region 2 field-aligned currents are associated. Proton aurora also contributes to ionospheric conductivities, which must be taken into account for accurate modeling of high latitude electrodynamics.

SAPS as defined by Foster and Burke [2002] refers to the broad, persistent, poleward-directed electric field which drives sunward plasma convection at sub-auroral latitudes in the evening local time sector. SAPS often appear in regions of low ionospheric conductivity equatorward of auroral electron precipitation during disturbed geomagnetic conditions. Currents driven into the sub-auroral ionosphere from the disturbed ring current put into play a sequence of magnetosphere-ionosphere coupling and feedback with dramatic consequences for the electric fields and particle populations of the Plasmasphere Boundary Layer.

The effects of SAPS in the ionosphere and magnetosphere include Storm Enhanced Density (SED), plumes of greatly enhanced ionospheric total electron content (TEC), erosion of the dusk-sector plasmasphere, and the formation of sunward-reaching plasmasphere drainage plumes. The inward extent of the SAPS electric field overlaps the outer plasmasphere on field lines mapping to the high-density cold plasmas equatorward of the ionospheric trough.

Subauroral flows have impact on mass redistribution in the coupled geospace system. Stormtime SAPS are associated with the enhanced asymmetric ring current and enhanced Region 2 current flows. During quiet times, SAPS occur in association with variable Bz conditions leading to enhanced convection, or they may be triggered by substorm activity. The exact relationship between SAPS and storm-enhanced densities are still now well understood. It represents a complex interplay between ionospheric production, loss, and transport.

Irregularities at VHF and UHF wavelengths are observed embedded in the SAPS flows at ionospheric altitudes. They may be created by two-stream Farley-Buneman field aligned irregularities, or by electric field variability in the polarization jet. Also, wave structures have been seen in the SAPS region, and thermospheric wind effects from strong ion-neutral coupling during SAPS westward flow forcing are also observed. Thermospheric poleward wind surges are often present at mid-latitudes during large magnetic storms.

Other phenomena occurring at subauroral latitudes are field-aligned, quasi-stationary (in the rotating frame) TEC ducts, created in the wake of a passing TID. Stable auroral red arcs are a common feature, but their relation to energy input from the ring current and precipitating energetic ions is not well understood.

Irregularities at mid-latitude at decameter wavelengths, triggered by either the gradient drift instability or temperature gradient instability are also present. These are quite important at HF wavelengths and drive all the subauroral scatter seen with the SuperDARN radars.

Incorporating the heater into the research enables experiments that would not be possible otherwise. Ionospheric modification experiments have tremendous potential for informing our investigation of the Earth's upper atmosphere, ionosphere, and magnetosphere. State parameters of the neutral gas in this region are difficult to measure with groundbased instruments, and the measurements that are possible are often poorly resolved in range or time or unavailable outside narrow altitude regimes. Neutral winds and densities in the thermosphere in particular are poorly specified, introducing uncertainty into virtually all lines of investigation in aeronomy. Since neutral winds and densities control satellite drag, their poor specification has important operational consequences. By exploiting the coupling between neutral and charged species, Ionospheric modification experiments allow us to measure neutral state parameters more systematically and over a broader range of conditions than would otherwise be possible.

The utility of ionospheric modification for understanding natural aeronomic processes is exemplified by research into polar summer mesospheric echoes (PMSE). PMSE refers to coherent radar scatter from thin layers in the polar summer mesosphere associated with polar mesospheric clouds. The echoes arise from fluctuations in electron density driven by atmospheric turbulence. Just how electron density fluctuations at small scale-sizes could be sustained in the presence of ordinary ambipolar diffusion was a daunting problem, which was resolved with the help of heating experiments. In these experiments, an overshoot in echo intensity was consistently observed after heater turnoff [Havness et al., 2003; Havness, 2004].
The overshoot led to an appreciation of multipolar diffusion, a fundamental but heretofore under-

appreciated process in multicomponent plasmas. Mahmoudian et al. [2011] accounted for the time history of the echoes in ionospheric modification experiments by modeling temperature dependent multipolar diffusion, charging, and recombination processes. The result was a substantial advance in our understanding of mesospheric turbulence, chemistry, and transport.

Below, some of the most promising techniques for exploring the Earth's upper atmosphere, ionosphere, and magnetosphere are described.

Neutral winds and densities, and energetic electrons using heater-induced airglow: Ionospheric modification experiments coupled with airglow observations can be used to estimate neutral density. The long radiative lifetime of O(1 D) means that its actual lifetime is controlled by collisional deactivation (quenching) which varies with the density of the neutral species in the thermosphere. Gustavsson et al. [2001] used a tomographic approach to estimate the decay time of O(1 D) excited in heating experiments as a function of altitude. Kalogerakis et al. [2009] went further, using the methodology to estimate density profiles of atomic oxygen, which they found dominates the quenching rate above about 200 km.

Combining RF heating with airglow imaging moreover offers a means of measuring neutral winds in the thermosphere. The method involves observing clouds of metastable O(1 D) atoms over the heater after heating is discontinued. During this time, these atoms drift with the neutral wind and expand under the influence of diffusion, all the time decaying by radiation and collisional quenching. On the basis of airglow imagery of bright, distinct clouds created by ionospheric modification, Bernhardt et al. [2012] were able to estimate the drift velocity, diffusion rate, and quenching rate of the O(1 D) atoms. They had, in effect, used ionospheric modification to perform a kind of repeatable chemical release experiment.

Neutral density and drifts, and electron densities from API: One of the most promising techniques for studying the background ionosphere and thermosphere involves so called "artificial periodic inhomogeneity", or API, which is based on ionospheric sounding [Belikovich et al., 1975; Fejer et al., 1984; Rietveld et al., 1996; Djuth et al., 1997; Bakhmet'eva and Belikovich, 2007]. In this technique, high-power RF heating is used to induce weak variations in the ionospheric index of refraction that follow the structure of the heating standing wave pattern. Horizontally-stratified, vertically-periodic structure is thus induced at altitudes from the D region (down to about 50 km) through the reflection height.

Once created, the ionospheric structure is diagnosed using HF sounding at frequencies calculated to match the probe signal to the pump standing wave pattern. The decay time of the structuring is measured as a function of altitude and taken to be indicative of the ambipolar diffusion rate in the E and F regions. (Below that, turbulent mixing and photochemistry dominate.) From the decay time constant, robust estimates of the neutral density can be formed. The measurement technique is straightforward, requires no true-height inversion, and functions in the valley region as well as the E and F regions. In the D region, electron number density can be measured from the Faraday rotation of the scattered probe signal, and complex photochemical and dynamical processes investigated.

Working at EISCAT, Rietveld et al. [1996] also examined the Doppler shift of the API backscatter and associated it with the vertical neutral wind in the D and lower E regions. They reported small (few m/s), zero-mean winds with signs of gravity wave fluctuations. This is a remarkable result, which holds the promise of very accurate vertical wind measurements in daylight as well as at night in over a range of altitudes not readily probed by other means.

Diffusion and cooling rates and E x B drifts: Coherent radar scatter from induced plasma density irregularities provides another diagnostic of background parameters in the mesosphere and thermosphere. A signature feature of ionospheric modification experiments is the generation of field-aligned plasma density irregularities (FAIs). The irregularities are generated mainly by thermal parametric instabilities [Grach et al., 1978; Das and Fejer, 1979; Fejer, 1979; Kuo and Lee, 1982; Dysthe et al., 1983; Mjolhus , 1990] and, having entered nonlinear stages of development, by resonance instability [Vas'kov and Gurevich , 1977; Inhester et al., 1981; Grach et al., 1981; Dysthe et al., 1982; Lee and Kuo, 1983; Mjolhus,1993]. These irregularities provide bright, regular targets of opportunity for coherent scatter radars, which can derive background information from them. Most research has concentrated on F region FAIs, although irregularities can be generated in the E region by pump waves with sufficiently low frequency.

The threshold pumpmode electric field required to excite FAI with a heater is a well-known function of many parameters including the electron cooling rate. By measuring this threshold in the E and F regions, estimates of the inelastic and elastic electron cooling rates can be derived.

The diffusion rate of FAIs can also be studied by monitoring how the coherent radar echoes decline in intensity after the heater is turned off. The decay timescale depends on the probe radar wavelength but is of the order of 100 ms for VHF radars in the E region and a few tens of seconds in the F region. Remarkably, the decay of the irregularities has been found to follow not one but two power laws: one fast, and one slow [Hysell et al., 1996]. The faster rate is consistent with ambipolar diffusion and consequently affords another estimate of the temperature, electron-neutral, and ion-neutral collision frequencies and composition at the ionospheric interaction height.

In addition to the backscatter power, the Doppler shift of the coherent echoes can also be measured during ionospheric modification experiments. Since the echoes have a much longer correlation time than incoherent scatter, the Doppler shifts can be measured far more accurately in a short time. In the Fregion, the Doppler shifts are indicative of E x B drifts. Heating experiments consequently afford extraordinarily accurate measurements of ionospheric electric fields using SuperDARN-class and similar radars even where natural ionospheric irregularities are not present.

Sporadic E layer morphology: Another example of discovery science in aeronomy facilitated by ionospheric modification concerns the morphology of sporadic E ionization layers. These layers, which were evident in the earliest days of radio, are often nonblanketing and patchy. The cause of the patchiness is enigmatic and difficult to research as conventional remote sensing instrumentation affords no simple means of obtaining imagery of the horizontal structure of the rapidly evolving and moving ionization layers.

Ionospheric modification experiments can be used to highlight natural structure in the sporadic E layers by making them visible to coherent scatter radar. The structure can be inferred through radar imaging techniques such as have been employed by Hysell et al. [2014]. Since field aligned irregularities are generated only in regions where the plasma frequency exceeds a threshold, varying the heating frequency can highlight different features in the layer structuring to the point of making truly three-dimensional imagery possible. This experimental technique produces images at a higher cadence and with better resolution than would be possible using incoherent scatter alone.

7. Application to Magnetospheric Physics

Although only 350 km south of Poker Flat, the HAARP location is conjugate to a distinctly different region of the magnetosphere. As discussed in Section 6, ionospheric dynamics over HAARP represent a projection of inner magnetospheric dynamics that drive phenomena such as proton aurora, radiation belt precipitation, and sub-auroral polarization streams (SAPS). The location has long supported experiments that directly probe the magnetosphere through active modification. For both active and passive research programs, the addition of AMISR and a comprehensive suite of supporting instruments will lead to a quantum leap forward in our understanding of several outstanding questions.

Substorms represent an impulsive release of inductive energy stored in Earth's magnetosphere. The mechanism of substorm triggering, the precise instability responsible for substorm expansion, and the cascade of energy release within the ionosphere-thermosphere system remain subjects of intense debate in both the aeronomy and magnetospheric communities.

Over the past decades, substorm research has evolved into a cross-disciplinary topic, with many impactful findings emerging from collaborative measurements from ground and space [e.g., Nishimura et al., 2010]. The PFISR facility and supporting optical measurements have provided invaluable space-time constraints in this research [Zou et al., 2010]. Ground-support of substorm and magnetospheric research does not fit neatly into a single program area; many of the Aeronomy topics discussed in Section 6 are direct projections of magnetospheric processes. The appreciation of substorm and magnetospheric research as cross-disciplinary topics will undoubtedly continue to grow. Just as the focus of NASA's heliophysics program has migrated from magnetotail (THEMIS) to radiation belts (Van Allen Probes) to solar wind - magnetosphere interactions (MMS), so is it appropriate for NSF's facilities program to migrate to different geomagnetic contexts (e.g., auroral oval to sub-auroral) to gain new perspectives on the coupled geospace system.

At L=5, Gakona is equatorward of the most likely latitude for substorm onsets, but still in a region that may play a significant role in the substorm process. As early as 1975 [Fukinishi, 1975] observations indicated that the electron arc that brightens at substorm onset is located very close to or within the region of proton aurora. An observatory at Gakona would enable overhead observation of the proton aurora and working in conjunction with the rest of the observational infrastructure in Alaska, would enable observation of the equatorward motion of arcs during the growth phase, and the interaction between the electron arcs and proton precipitation. An ISR located at Gakona would augment these observations to provide detailed

information on the plasma flows around the arcs and help to determine the structure of the field-aligned current and magnetosphere-ionosphere coupling.

One of the benefits of Gakona's location is that it permits direct probing of the magnetosphere with heater generated ELF and VLF waves. Unlike the EISCAT Tromso heater, which was located at L > 6 and thus often on open geomagnetic field lines, the Gakona facility is at L =4.9 where geomagnetic field lines are usually dipole-like and tend to lie within or near the plasmaspause. HAARP is thus well positioned for use in controlled wave-injection experiments to study ELF/VLF wave growth and emission triggering, induced

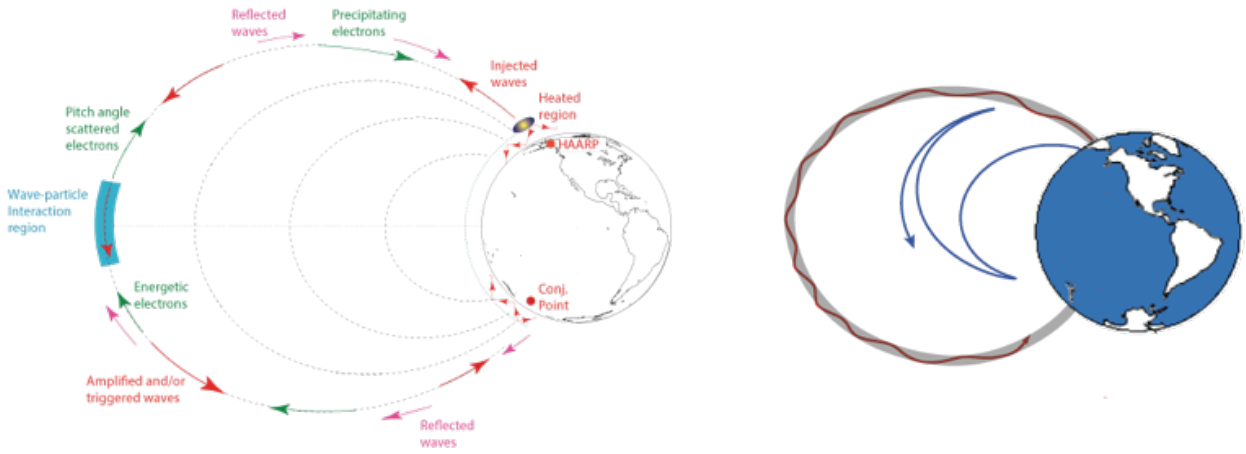

Figure 8. (Left) schematic of whistler mode wave injection experiments where ELF/VLF waves generated in the ionosphere are injected into the Earth-ionosphere waveguide and the magnetosphere. Waves in the magnetosphere undergo amplification upon interaction with radiation belt electrons. Electrons are pitch angle scattered and precipitated. (Right) propagation of whistler mode waves in the ducted (red) and non-ducted (blue) mode. Non-ducted waves undergo magnetospheric reflections and are typically only observable on spacecraft.

energetic particle precipitation and propagation of whistler mode waves. All of these processes are key drivers of magnetospheric energy dynamics and space weather effects with direct impact on a large body of current research efforts. For example, nonlinear cyclotron resonance theories describing naturally occurring hiss and chorus emissions are the same as (and were initially derived for) emissions induced by controlled ELF/VLF sources. Figure 8 illustrates the concept of magnetospheric probing with heater induced ELF/VLF waves. As shown in the right panel of the figure, the heater can excite whistler mode waves that propagate both in the ducted and non-ducted modes in the magnetosphere.

Numerous techniques have been developed for optimizing ELF/VLF generation in terms of amplitude, directionality and preferential coupling into the magnetosphere *[Cohen et al., 2008, 2010, 2011; Golkowski et al, 2011; Moore and Agrawal, 2011; Papadapoulos et al, 2011].*

Many of these techniques remain to be fully exploited in investigating key magnetospheric physics issues described below.

Magnetospheric amplification of ELF/VLF waves: The Gakona facility remains the only dedicated science facility able to excite the cyclotron resonance instability in the magnetosphere that is the driver of all whistler mode waves in near-Earth space. Controlled wave injection experiments with ground based observations in the local and conjugate hemisphere were pioneered at Siple Station in Antarctica (1973-1988)[*Heliwell*, 1988] and then successfully expanded using the HAARP heater [*Inan et al, 2004; Golkowski et al.*, 2008, 2009, 2010, 2011]. Despite the lower power of generated ELF/VLF waves via ionospheric current modulation as compared to the conventional Siple Station 150 kW transmitter, using the heater offers the advantages of unprecedented frequency- time flexibility. Key outstanding questions to be explored include: 1) under what conditions are whistler mode waves most likely to be amplified, 2) what are the coherence limits of amplification, 3) what are the dynamics of the hot electron distribution during amplification.

Precipitation of radiation belt electrons: In parallel with and even more prevalent than amplification of heater induced whistler mode waves is the effect of generated waves on energetic electron trajectories i.e. "particle precipitation" where energetic particles have their trajectories modified to impinge on the ionosphere and be lost from the radiation belts. Quasi-linear theory and effective diffusion coefficients [*Inan et al.,* 1978*; Abel and Thorne,* 1998*; Albert,* 1999*; Summers,* 2005] has been the most common approach to treating this process even though recent works have highlighted that non-linear effects become apparent at lower amplitudes than previously predicted [*Harid et al.*, 2014]. Detection and quantification of precipitation is often challenging. The most straightforward observations are from spacecraft with particle detectors that are able to differentiate particle pitch angles and make simultaneous observations of wave amplitudes. However, spacecraft quickly fly through large scale dynamic environments where the wave characteristics and particle populations are both changing. Ground based techniques include VLF remote sensing, optical observations, and incoherent scatter radar. In this context, the addition of an ISR at Gakona would be an excellent asset in controlled precipitation studies. A repetitive wave injection format would create a secondary ionization response in the ionosphere that could be observed with the ISR. Efforts were made in 2009 on such an experiment using the PFISR facility, but results were inconclusive due to unfavorable location of PFISR. Fundamental questions to be explored include: 1) what is the role of ground based ELV/VLF sources in controlling radiation belt populations 2) Is quasi-linear theory best toll to predict radiation belt lifetimes, 3) are there optimal frequency-time formats for maximizing electron precipitation for a given wave amplitude.

Propagation of whistler mode waves and spacecraft observations: Even the passive propagation of whistler mode waves in near-Earth space is not analytically tractable and requires numerical models. Field aligned density irregularities and the plasmapause boundary itself are known to guide waves and confine wave energy to the geomagnetic field line. However, the prevalence of these structures and their role in a large class of whistler mode phenomena remains disputed [*Haque et al.*, 2011]. Numerical models typically assume one of two extremes: fully guided field aligned modes, or a smooth background plasma density, which allows for a WKB approximation and raytracing solution. A controlled ELF/VLF source from which waves can be observed on spacecraft offers a way to validate models and improve fundamental understanding.

Numerous existing and planned spacecraft have instruments that can observe ELF/VLF waves generated in the ionosphere above Gakona. These include the Van Allen Probes (NASA- active), CASSIOPE (Canada- active), ERG (Japan - planned), and DSX (US Air Force - planned). Likewise, it is important to note that there have been suggestions that the heater itself can generate density irregularities for guiding waves [*Vartanyan et al.*, 2012; *Woodroffe et al.*, 2013]. Whether these structures can be reliable created or are mostly naturally occurring [*Piddyachiy et al.*, 2011] is an important question for future investigation. Moreover, there is no doubt that both the wave amplification and electron precipitation research efforts discussed above would gain considerably with simultaneous spacecraft observations. To provide just one example, observation of triggered waves in the non-ducted mode is expected to be possible only with spacecraft and can answer the question of how prevalent is the process when whistler mode waves are oblique and not field-aligned.

Ionospheric conductances and M/I coupling: When mircopulsations are present, the electric fields inferred from coherent scatter is indicative of the electric fields of the Alfven waves that carry them. Such micropulsations are frequently observed over the Sura heater [*Yampolski et al.*, 1996]. Remarkably, Sinitsin et al. [1997] measured the Doppler shifts of heaterinduced FAIs over Sura at three different places along a single magnetic flux tube and found that the three signatures could not be accounted for by a single shear Alfven wave. Attributing the signatures to and incident shear wave, a reflected shear wave, and a reflected magnetosonic wave, they were able to infer the Pedersen and Hall conductances at the foot of the flux tube. This is a unique experimental capability with tremendous value for MI coupling studies with the potential to provide dynamic lower boundary conditions for magnetospheric models in real time.

8. Application to Radio Science and space-based navigation and communication

The ionospheric disturbances produced in heating experiments have practical application to understanding space weather effects of natural ionospheric disturbances. As a source of localized plasma enhancements or field-aligned density irregularities, HAARP can be used for controlled experiments to measure ionospheric effects on radio signals. A recently published example [*Bernhardt et al.*, 2016] of strong scintillation of satellite-to-ground signals from the TACSat4 spacecraft showed over 15 dB of fading produced by the HAARP generated irregularities. Experiments can be used to further our understanding of ionospheric impacts and can be used to test mitigation strategies.

HAARP can be used for research on ionospheric effects on HF over-the-horizon radars in two types of experiments. First, it can be used as a controlled source of ionospheric irregularities to quantify their impacts. Since the Kodiak radar observes the region over HAARP, and functions in the same manner as an Arctic OTH Radar, it can be used to quantify the effects of irregularities, and can serve as a testbed for mitigation algorithms. Additionally, precisely-timed D-region heating experiments can be used to change the received frequency of HF signals propagating through the heated region, affecting OTH processing of the signals, as demonstrated by Langston and Moore [2013]. The second type of experiments will use the HAARP transmitter in a mode to simulate an OTH Radar transmitter, and use the Kodiak radar as the receive array. Those experiments would employ a range of modulations of the transmitter to test MIMO techniques for mitigation of ionospheric effects.

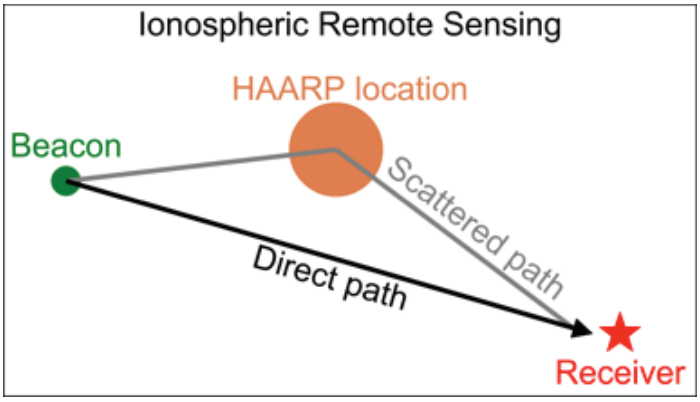

Figure 9. Illustration of the impact of ionospheric disturbances on radio paths.

How does the ionosphere impact radio communications during active and disturbed conditions? HAARP can also be used to quantify the impact of ionospheric disturbance on ground radio communications. Figure 9 shows schematically how this is performed. There are numerous radio beacons ranging from 10 kHz up to 10 MHz all of which propagate to long distances via reflection or refraction from the ionosphere. When HAARP heats up the ionosphere it forms *a controllable* disturbed patch. We can control the power level, beam direction, HF frequency and mode, etc. This disturbed patch in the ionosphere can scatter the transmitter signal, which is then picked up at a distant receiver. By moving the location of the HAARP heated region, we can study the scattering pattern of the ionospheric disturbance and therefore quantify the impact of external drives from natural sources on radio propagation.

9. Application to ELF/VLF communication and navigation

Extremely low frequency (ELF, 3-3000 Hz) and very low frequency (VLF, 3-30 kHz) waves can propagate to global distances with low attenuation and penetrate deeply into seawater [e.g., Keiser, 1974; Wait, 1977; Bannister, 1984]. Thus, ELF/VLF waves are ideal for long-distance communications with submerged vehicles [e.g., Bernstein et al., 1974; Merrill, 1974], for global navigation applications [e.g., Swanson, 1983; Frank, 1983; Inan et al., 1985], and for remote sensing of the ionosphere [e.g., Cummer et al., 1998; Dowden et al., 2002]. Conventional methods to broadcast electromagnetic waves in the lower range of the ELF/VLF band (i.e., <5 kHz), however, are typically costly and inefficient (on the order of ~0.1%) [Raghuram et al., 1974; Barr et al., 1985]. ELF/VLF wave generation by modulated high frequency (HF, 3-30 MHz) heating of the ionosphere thus represents an important alternative source for ELF/VLF waves [e.g., Papadopoulos et al., 1990; Barr et al., 1991; Cohen et al., 2012].

What is Special about HAARP ELF/VLF Generation? HAARP's HF transmitter has unique capabilities for generating ELF/VLF waves. Other ionospheric heaters (and HAARP) can control the HF power, HF polarization, and modulation frequency [e.g., Ferraro et al., 1984; Barr et al., 1991a; Barr et al., 1991b; Villasenor et al., 1996; Milikh et al., 1999; Moore et al., 2006]. The versatility of the HAARP transmitter is what sets it apart, however. It can precisely control the modulation waveform, it has dual-beam transmission capabilities, and it can rapidly direct and re-direct the beams in different directions with 10 microsecond cadence. These capabilities allow HAARP ELF/VLF wave generation experiments to investigate 1) exotic methods to improve ELF/VLF wave generation efficiency, 2) interferometric methods to identify the phase center of the ionospheric source, and 3) basic plasma physics by quantifying the relative importance of different nonlinear interactions in the ionosphere.

Improving ELF/VLF Wave Generation Efficiency: Prior to HAARP's shutdown period, great strides were made improving ELF/VLF wave generation efficiency. Cohen et al. [2008] identified "Geometric Modulation" (GM), or rapidly moving the heater beam with an ELF/VLF repetition rate, as a means to increase wave generation efficiency by 7-11 dB. Fujimaru [2014] optimized the GM source by combining it with a beam painting technique, accounting for experimentally measured heating/cooling rates and the propagation delay to different heating spots, and attained an additional efficiency improvement of 7-11 dB. While tremendous (14-22 dB improvements) have been made, it is unclear what geometric shape optimizes the ELF/VLF source (only circles and lines have been explored so far), and it is unclear whether clever use of multiple beams at different frequencies can control the directionality of the source.

Impacting Global Navigation Solutions: Ongoing efforts to reproduce GPS-accurate navigation and timing solutions using ELF/VLF signals are significantly limited by the bandwidth of conventional VLF transmitters. ELF/VLF waves generated at HAARP do not suffer from such bandwidth limitations, but instead suffer from the fact that the ELF/VLF source currents in the ionosphere vary with time (resulting in a time-varying, frequency-dependent phase center). Recent efforts by Payne [2007] attempted to quantify the spatial and temporal variation of the ionospheric currents using interferometric methods applied to CW ELF/VLF waves, without success. Fujimaru and Moore [2011] used a chirped ELF/VLF waveform, however, to identify altitude of the ELF/VLF source using only a single receiver. It is conceivable that clever modulation formats and techniques may be used to quantify the spatio-temporal distribution of ELF/VLF source currents in the ionosphere or at least identify the location of the phase center.

Experimentally Quantifying Nonlinear Wave-Plasma Interactions: HAARP's versatility is imperative to studying wave-plasma interactions in the D-region ionosphere. By modulating the beams in different ways, HAARP's dual-beam transmission capability can be used to transmit a large variety of signal components at different frequencies that have the potential to interact with the plasma and with each other (via the plasma). Careful control of these signals yields the ability to quantify the relative importance of different nonlinear interactions. For example, Agrawal and Moore [2012] studied how a CW beam could be used to suppress the amplitude of the ELF/VLF wave generated by second modulated beam. Additionally, Moore et al. [2013] presented evidence that ELF/VLF waves were generated by the 3-step excitation of the thermal cubic nonlinearity. A wide variety of wave-wave and wave-plasma interactions have yet to be explored and quantified

10. Practical aspects (costs, ISR options)

With no current federal sponsor, HAARP is being operated by the University of Alaska Geophysical Institute using internal UAF funds. UAF will continue this support for a period of about two years after which we will evaluate the status and potentially cease operations if it does not appear that sponsors will be forthcoming. Until that time we are charging user fees for any operation. The fees will be based upon the actual costs and an assumed number of hours of operation in the next year. Initially we have set the rate at $5000 per hour of heater operation, which is below the costs expected for the first few years of operation.

Estimates for operating costs are based upon fixed costs of about $1.3M (personnel, utilities, custodial, telephone, internet, equipment and supplies, and travel), additional variable costs of about $2000 per hour of heater operations, and institutional overhead of 26%. Hence, about 660 hours of operation at the set rate are required for UAF to cover costs.

An alternative funding model with potentially lower total cost of operation would be for an agency to provide a base of funding of $1.5M, then the hourly fee charged would only have to cover the variable costs. Under this funding model, UAF would break even with only a few hours of operation.

AMISR Deployment options: Many of the scientific objectives described above require the deployment of an ISR to Gakona. Advanced Modular Incoherent Scatter (AMISR) systems are active phased-array radars composed of individual antenna element units (AEUs) organized in panels of 32 AEUs each. Each AEU has its own transmitter capable of 500 W, and the panels are designed to be reconfigurable and relocatable. Currently the NSF supports a 128-panel AMISR in Poker Flat, Alaska (PFISR) and a 121-panel AMISR in Resolute Bay, Canada (RISR-N). There is also a smaller 16-panel system at Gakona (MUIR) and a 14-panel system at the Jicamarca Radio Observatory in Peru (UMET-14).

Three options for deploying an AMISR to Gakona are:
1. Build a new 96-panel or 128-panel radar in Gakona.
2. Redeploy existing panels from PFISR, RISR-N, MUIR, and UMET-14 to assemble an 87-panel radar in Gakona.
3. Relocate all 128 PFISR panels to Gakona.

Regardless of where the panels come from, all of these options would require building a new steel structure to receive the panels, preparing the existing pad at the site, and providing prime power to the site.

The first option is the most desirable option. It creates a sensitive radar in Gakona, it preserves all the existing capabilities of the other AMISRs, and it permits coordinated studies using both the Gakona ISR (GISR) and PFISR.

The second option would assemble an 87-panel GISR using 32 panels from PFISR (leaving 96 at PFISR), 25 panels from RISR-N (leaving 96 at RISR-N), all 16 MUIR panels, and all 14 UMET-14 panels. This plan would maintain PFISR operations and allow coordinated studies using both GISR and PFISR. In this plan the 96 panels left at PFISR would be refurbished to ensure the continued viability of a 96-panel PFISR, and all of the panels shipped to Gakona would be refurbished before combining them. Nonetheless, the resultant 96-panel PFISR, 96-panel RISR-N, and 87-panel GISR would all be less sensitive than PFISR and RISR-N are currently. This option would also terminate the coherent scatter studies of equatorial electrojet and equatorial spread-F being conducted with the UMET-14 radar.

The third option would move the PFISR to Gakona, resulting in a high-quality radar at Gakona but the complete termination of PFISR operations. This would mean a loss of the ability to support sounding rocket launches from the Poker Flat Research Range (PFRR), loss of the coordination between PFISR and the other clusters of instruments at PFRR, and a termination of the nearly continuous dataset that has been collected since 2007.

In this scenario there would be at least 3 months of down time while the panels were being moved when neither PFISR nor GISR could be operated. Unlike the previous two options, this option does not permit coordinated radar studies with both PFISR and GISR.

When quantifying the performance of an AMISR, the statistical certainty of a measurement scales like the product between the transmit power, the receiver area, and the square root of the number of pulses averaged. Dividing an AMISR into a smaller number of panels and decreasing the power-aperture product (PA) forces one to either increase the integration time and/or decrease the number of pointing positions, thereby limiting its scientific utility. A full 128-panel AMISR is theoretically capable of 2 MW of transmit power, or a PA of 256 MW-panels, however neither PFISR nor RISR-N have ever achieved the full 2 MW since not every AEU will deliver the full 500 W. Today PFISR and RISR-N have an approximate PA of 170 MW-panels. The tables below compare the relative performance of the PFISR, RISR-N, and GISR under the three options presented above. The fourth option in the table assumes that a radar will not be placed in Gakona, but instead the PFISR and RISR-N will be refurbished and left in place. All of the numbers assume the panels will be refurbished such that the AEUs transmit 90% of their maximum 500 W on average. The time factors quoted in the bottom rows are the amount of time one would need to integrate to get the same statistical certainty as present day PFISR.

PFISR	Current	1	2	3	4
Tx Power (MW)	1.35	1.8	1.38	0	1.8
Rx Panels	128	128	96	0	128
PA (MW-panels)	173	230	132	0	230
Time Factor*	1.0	0.56	1.72	infinity	0.56
RISR-N	**Current**	**1**	**2**	**3**	**4**
Tx Power (MW)	1.4	1.74	1.38	1.74	1.74
Rx Panels	121	121	96	121	121
PA (MW-panels)	169	211	132	211	211
Time Factor*	1.05	0.67	1.72	0.67	0.67
GISR	**Current**	**1**	**2**	**3**	**4**
Tx Power (MW)	0	1.38	1.25	1.8	0
Rx Panels	0	96	87	128	0
PA (MW-panels)	0	132	109	230	0
Time Factor*	infinity	1.72	2.52	0.56	infinity

Costing information: Over the period of 2003 to 2009, SRI designed , produced and deployed 128 panel AMISRs at Poker Flat and, Resolute Bay and prepared the site, and erected the structure for RISR-C These efforts were funded be NSF under the AMISR project and cost on the order of $50M. One could make estimates of the cost of producing GISR from these historical numbers. In addition, a few years ago when the idea of relocating AMISRs to locations like Gakona, Argentina etc. was being pursued by NSF, costs were estimated with the assumptions that the host location would prepare a suitable site, procure and erect the appropriate structure, provide power and internet connectivity. The costs of moving panels and utility distribution units varied from about $1-2M depending on location. All of these costs need to be updated with current pricing in order to be useful for budgetary purposes.

11. Conclusions

This report makes the case for supporting research in the sub-auroral region by establishing a year-round observatory at the location of the HAARP facilities in Gakona, Alaska. The region of space accessible from Gakona is underexplored and provides excellent opportunities for discovery science. There has never been a CEDAR Class 1 facility directly below the sub-auroral ionosphere, which has limited our ability to examine the mesosphere-lower-thermosphere (MLT), and the D-region and E-region ionosphere, where the most critical magnetosphere-ionosphere-atmosphere coupling processes take place. There are many unique features of this region of geospace that remain to be explored. Only recently have we begun to realize the linkage of the region to phenomena occurring at higher latitudes and its importance in the system-like behavior of geospace. Establishing the observatory at Gakona will help us toward achieving full understanding of the entire space weather system.

A central aspect of our observatory vision will be continued research using the HAARP high-power HF transmitter to explore atmospheric, ionospheric, and magnetospheric physics. The breadth of topics described in this report demonstrates the unique contributions HAARP will make to each of these area. Several of the topics described cannot be studied by other means. Further the ability of ionospheric heaters to execute controlled repeatable experiments is unique to geospace research, and has outstanding promise for systematically establishing several fundamental physical parameters.

Finally, the importance of establishing an incoherent-scatter radar (ISR) at the observatory cannot be overstated. The observatory could not be considered a true CEDAR class-1 facility without one. Nearly every research topic envisioned for the observatory will be enhanced by an ISR. Some of the topics described can be studied only with an ISR. The configuration described in this report with ISRs located at both Poker Flat (PFISR) and Gakona (GISR) will provide an observing geometry that has not existed previously. It would enable simultaneous observations of both the auroral zone and the sub-auroral zone, which is required for unraveling the role of the inner magnetosphere in the substorm process.

Contributors

Paul Bernhardt, Naval Research Laboratory
William Bristow, University of Alaska Fairbanks
Morris Cohen, Georgia Institute of Technology
Philip Erickson, MIT Haystack Observatory
Christopher Fallen, University of Alaska Fairbanks
Mark Golkowski, University of Denver
Don Hampton, University of Alaska Fairbanks
David Hysell, Cornell University
John Kelly, SRI International
Elizabeth Kendall, SRI International
Robert Michell, University of Maryland
Robert Moore, University of Florida
Jade Morton, University of Colorado Boulder
Robert Robinson, InSpace Inc.
Wayne Scales, Virginia Polytechnic University
Joshua Semeter, Boston University
David Suszcynsky, Los Alamos National Laboratory
Roger Varney, SRI International

References

Abel, B., and R. M. Thorne (1998), Electron scattering loss in Earth's inner magnetosphere: 1. Dominant physical processes, J. Geophys. Res. , 103, 2385–2396, doi:10.1029/97JA02919.

Adeishvili, T. S., A. V. Gurevich, S. B. Liakhov, G. G. Managadze, G. M. Milikh, and I. S. Shliuger, Ionospheric emission caused by an intense radio wave, Soviet Journal of Plasma Physics, 4, 1293–1301,Nov.–Dec., 1978.

Agrawal, D., and R. C. Moore (2012), Dual-beam ELF wave generation as a function of power, frequency, modulation waveform, and receiver location, J. Geophys. Res., 117, A12305, doi:10.1029/2012JA018061.

Bakhmet'eva, N. V., and V. V. Belikovich, Modification of the earth's ionosphere by high-power HF radio emission: Artificial periodic inhomogeneities and the sporadic E layer, Radiophys. Quant. Elect., 50, 633–644, 2007.

Bannister, P. (1984), ELF propagation update, IEEE J. Oceanic Eng., 9(3), 179-188, doi:0.1109/JOE.1984.1145609.

Barr, R., M. T. Rietveld, H. Kopka, P. Stubbe, and E. Nielsen (1985), Extra-low-frequency radiation from the polar electrojet antenna, Nature, 317, 155-157, doi:10.1038/317155a0.

Barr, R., and P. Stubbe (1991a), ELF radiation from the Tromso "Super Heater" Facility, Geophys. Res. Lett., 18(6), 1035-1038, doi:10.1029/91GL01156.

Barr, R., and P. Stubbe (1991b), On the ELF Generation Efficiency of the Tromso Heater Facility, Geophys. Res. Lett., 18(11), 1971-1974, doi:10.1029/91GL02544.

Barr, R., P. Stubbe, and H. Kopka (1991c), Long-range detection of VLF radiation produced by heating the auroral electrojet, Radio Sci., 26(4), 871-879, doi:10.1029/91RS00777.

Belikovich, V. V., E. A. Benediktov, G. . G. Getmantsev, Y. A. Ignat´ev, and G. P. Komrako, Scattering of radio waves from the artificially perturbed F region, JETP Lett., Engl. Transl., 22, 243–244, 1975.

Bernhardt, P. A., M. Wong, J. D. Huba, B. G. Fejer, L. S. Wagner, J. A. Goldstein, C. A. Selcher, V. L. Frolov, and E. N. Sergeev, Optical remote sensing of the thermosphere with HF pumped artificial airglow, J. Geophys. Res. , 105 , DOI: 10.1029/1999JA000,366, 2012.

Bernhardt, P. A., C. A. Tepley, and L. M. Duncan, Airglow enhancements associated with plasma cavities formed during ionospheric heating experiments, J. Geophys. Res., 94 , 9071–9092, 1989.

Bernstein, S. L., M. L. Burrows, J. E. Evans, A. S. Griffiths, D. A. McNeill, C. W. Niessen, I. Richer, D. P. White, D. K. Willim (1974), Long-range communications at extremely low frequencies, Proceedings of the IEEE, 62(3), 292-312, doi: 110.1109/PROC.1974.9426.

Biondi, A. A., D. P. Sipler, and R. D. Hake, Optical _ -6300 detection of radio frequency heating of electrons in the F region, J. Geophys. Res., 75 , 6421–6424, 1970.

Burch, J. L., et al. (2002), Interplanetary magnetic field control of after-noon-sector detached proton auroral arcs, J. Geophys. Res., 107(A9), 1251, doi:10.1029/2001JA007554.

Carlson, H., V. Wickwar, and G. Mantas, Observations of fluxes of suprathermal electrons accelerated by HF excited instabilities, J. Atmos. Terr. Phys. , 44(12) , 1089–1100, 1982.
Das, A. C., and J. A. Fejer, Resonance instability of small-scale field-aligned irregularities, J. Geophys. Res., 84, 6701–6704, 1979.

Cohen, M. B., U. S. Inan, and M. A. Golowski (2008), Geometric modulation: A more effective method of steerable ELF/VLF wave generation with continuous HF heating of the lower ionosphere, Geophys. Res. Lett., 35, L12101, doi:10.1029/2008GL034061.

Cohen, M. B., M. Golkowski, N. G. Lehtinen, U. S. Inan, and M. J. McCarrick (2012), HF beam parameters in ELF/VLF wave generation via modulated heating of the ionosphere, J. Geophys. Res., 117, A05327, doi:10.1029/2012JA017585.

Cummer, S. A., U. S. Inan, and T. F. Bell (1998), Ionospheric D region remote sensing using VLF radio atmospherics, Radio Sci., 33(6), 1781-1792, doi:10.1029/98RS02381.

Dahlgren, H., J. L. Semeter, R. A. Marshall, and M. Zettergren (2013), The optical manifestation of dispersive field-aligned bursts in auroral breakup arcs, J. Geophys. Res. Space Physics, 118, 4572–4582 doi:10.1002/jgra.50415.

Djuth, F. T., K. M. Groves, J. H. Elder, E. R. Shinn, J. M. Quinn, J. Villasenor, and A. Y. Wong, Measurements of artificial periodic inhomogeneities at HIPAS Observatory, J. Geophys. Res. , 102 , 24,023–24,035, 1997.

Djuth, F. T., T. R. Pedersen, E. A. Gerken, P. A. Bernhardt, C. A. Selcher, W. A. Bristow, and M. J. Kosch, Ionospheric modification at twice the electron cyclotron frequency, Phys. Rev. Lett., 94, 125,001–1–4, 2005.

Dowden, R. L., J. B. Brundell, and C. J. Rodger (2002), VLF lightning location by time of group arrival (TOGA) at multiple sites, J. Atmos. Solar-Terr. Phys., 64(7), 817-830, doi:10.1016/S1364-6826(02)00085-8.

Dysthe, K., E. Mjølhus, H. P´ecseli, and K. Rypdal, A thermal oscillating two-stream instability, Phys. Fluids, 26 , 146, 1983.

Fejer, J. A. (1955), The interaction of pulsed radio waves in the ionosphere, Journal of Atmospheric and Terrestrial Physics, 7, 322-332.

Fejer, J. A., Ionospheric modification and parametric instabilities, Rev. Geophys. Space Phys., 17 , 135–153, 1979.

Fejer, J. A., F. T. Djuth, and C. A. Gonzalez, Bragg backscatter from plasma inhomogenieties due to a powerful ionospherically reflected radio wave, J. Geophys. Res. , 89 , 9145, 1984.
Grach, S., N. Mityakov, V. Rapoport, and V. Trakhtengertz, Thermal parametric turbulence in a plasma, Physica , D, 2 , 102–106, 1981.

Fejer, J. A. (1970), Radio wave probing of the lower ionosphere by cross-modulation techniques, Journal of Atmospheric and Terrestrial Physics, 32, 597-607.
Dysthe, K., E. Mjølhus, H. P´ecseli, and K. Rypdal, Thermal cavitons, Phys. Scr. T., 2 , 548–559, 1982.

Ferraro, A. J., H. S. Lee, R. Allshouse, K. Carroll, R. Lunnen, and T. Collins (1984), Characteristics of ionospheric ELF radiation generated by HF heating, J. Atmos. Terr. Phys., 46, 855-865.

Foster, J. C., and W. J. Burke (2002), SAPS: A new categorization for sub-auroral electric fields, Eos Trans. AGU, 83(36), 393–394, doi:10.1029/2002EO000289.

Frank, R. L. (1983), Current developments in LORAN-C, Proc. IEEE, 71, 1127.

Fujimaru, S. (2014), Optimization of beam painting for ELF/VLF wave generation at HAARP using time-of-arrival analysis, Ph.D. thesis, University of Florida, Gainesville, Florida, USA.

Fujimaru, S., and R. C. Moore (2011), Analysis of time-of-arrival observations performed during ELF/VLF wave generation experiments at HAARP, Radio Sci., 46, RS0M03, doi:10.1029/2011RS004695.

Fukunishi, H. (1975), Dynamic relationship between proton and electron auroral substorms, J. Geophys. Res., 80(4), 553–574, doi:10.1029/JA080i004p00553.

Gołkowski, M., U. S. Inan, A. R. Gibby, and M. B. Cohen (2008), Magnetospheric amplification and emission triggering by ELF/VLF waves injected by the 3.6 MW HAARP ionospheric heater, J. Geophys. Res.,113, A10201, doi:10.1029/2008JA013157.

Golkowski, M., U. S. Inan, and M. B. Cohen (2009), Cross modulation of whistler mode and HF waves above the HAARP ionospheric heater, Geophys. Res. Lett., 36, L15103, doi:10.1029/2009GL039669.

Gołkowski, M., U. S. Inan, M. B. Cohen, and A. R. Gibby (2010), Amplitude and phase of nonlinear magnetospheric wave growth excited by the HAARP HF heater, J. Geophys. Res. ,115, A00F04, doi:10.1029/2009JA014610.

Gołkowski, M., M. B. Cohen, D. Carpenter, and U. Inan (2011), On the occurrence of ground observations of ELF/VLF magnetosphericamplification induced by the HAARP facility, J. Geophys. Res.,116, A04208, doi:10.1029/2010JA016261.

Grach, S. M., A. N. Karashtin, N. A. Mityzkov, V. O. Rapoport, and V. Y. Trakhtengerts, Theory of thermal parametric instability in an inhomogenous plasma, Sov. J. Plasma Phys. (Engl. Transl.), 4, 737–741, 1978

Gurevich, A. V., Nonlinear effects in the ionosphere, Uspekhi Fizicheskikh Nauk. , 177(11), 1145–1177, 2007.

Gustavsson, B., and B. Eliasson, HF radio wave acceleration of ionospheric electrons: Analysis of HF-induced optical enhancements, J. Geophys. Res. , 113. A08319, doi:10.1029/2007JA012,913, 2008.

Gustavsson, B., B. U. E. Br¨andstr¨om, °A. Steen, T. Sergeinko, T. B. Leyser, M. T. Rietveld, T. Aso, and M. Ejiri, Nearly simultaneous images of HF-pump enhanced airglow at 6300 °A and 5577 °A, Geophys. Res. Lett. , 29 , doi:10.29/2002GL015,350, 2003.

Gustavsson, B., et al., First tomographic estimate of volume distribution of enhanced airglow emission caused by HF pumping, J. Geophys. Res. , 106 , 29,105–29,123, 2001a.
Gustavsson, B., et al., First tomographic estimate of volume distribution of HF-pump enhanced airglow emission, J. Geophys. Res., 106, 29,105–29,124, 2001b.

Gustavsson, B., et al., The electron distribution during HF pumping, a picture painted with all colours, Ann. Geophys. , 23 , 1747–1754, 2005.

Haque, N., U. S. Inan, T. F. Bell, J. S. Pickett, J. G. Trotignon, and G. Facskó (2011), Cluster observations of whistler mode ducts and banded chorus, Geophys. Res. Lett.,38, L18107, doi:10.1029/2011GL049112

Harid,V.,M.Gołkowski,T.Bell,and U.S.Inan (2014), Theoretical and numerical analysis of radiation belt electron precipitation by coherent whistler mode waves,J. Geophys. Res. Space Physics,119, doi:10.1002/2014JA019809

Haslett, J. C., and L. R. Megill, A model of the enhanced airglow excited by RF radiation, Radio Sci., 9,1005–1019, 1974.

Havness, O., Polar Mesospheric Summer Echoes (PMSE) overshoot effect due to cycling of artificial electron heating, J. Geophys. Res. , 109 , doi:10.1029/2003JA010,159, 2004.

Havness, O., C. L. Hoz, and L. L. Naesheim, First observations of the PMSE overshoot effect and its use for investigating the conditions in the summer mesosphere, J. Geophys. Res., 30, 2229, 2003.

Helliwell, R. A. (1988), VLF wave stimulation experiments in the magnetosphere from Siple station, Antarctica, Rev. Geophys.,26 (3), 551–578, doi:10.1029/RG026i003p00551

Huxley, L. G. H., and J. A. Ratcliffe (1949), A survey of ionospheric cross-modulation, Proc. Inst. Elec. Eng., 96, 433-440.

Hysell, D. L., M. C. Kelley, Y. M. Yampolski, V. S. Beley, A. V. Koloskov, P. V. Ponomarenko, and O. F. Tyrnov, HF radar observations of decaying artificial field aligned irregularities, J. Geophys. Res., 101, 26,981, 1996.

Hysell, D. L., R. H. Varney, M. N. Vlasov, E. Nossa, B.Watkins, T. Pedersen, and J. D. Huba, Estimating the electron energy distribution during ionospheric modification from spectrographic airglow measurements, J. Geophys. Res. , 117 , doi:10.1029/2011JA017, 18, 2012.

Hysell, D. L., M. J. McCarrick, C. T. Fallen, and J. Vierinen, First artificial periodic inhomogeneity experiments at HAARP, Geophys. Res. Lett. , 42 , 1297–1303, doi:10.1002/2015GL063,064, 2014a.

Hysell, D. L., R. J. Miceli, E. A. Kendall, N. M. Schlatter, R. H. Varney, B. J. Watkins, T. R. Pedersen, P. A. Bernhardt, and J. D. Huba, Heater-induced ionization inferred from spectrometric airglow measurements, J. Geophys. Res. , 119 , 2038–2045, DOI: 10.1002/2013JA019,663, 2014b.

Hysell, D. L., J. Munk, and M. McCarrick, Sporadic E ionization layers observed with radar imaging and ionospheric modification, Geophys. Res. Lett. , 41 , DOI:10.1002/2014GL061,691, 2014c.

Inan, U. S., T. F. Bell, and R. A. Helliwell (1978), Nonlinear pitch angle scattering of energetic electrons by coherent VLF waves in the magnetosphere, J. Geophys. Res. ,83 (A7), 3235–3253, doi:10.1029/JA083iA07p03235.

Inan, U. S., D. L. Carpenter, R. A. Helliwell, and J. P. Katsufrakis (1985), Subionospheric VLF/LF phase perturbations produced by lightning-whistler induced particle precipitation, J. Geophys. Res., 90(A8), 7457-7469, doi:10.1029/JA090iA08p07457.

Inhester, B., A. C. Das, and J. A. Fejer, Generation of small-scale field-aligned irregularities in ionospheric heating experiments, J. Geophys. Res. , 86 , 9101–9105, 1981.

Kalogerakis, K. S., T. G. Slanger, E. A. Kendall, T. R. Pedersen, M. J. Kosch, B. Gustavsson, and M. T. Rietveld, Remote oxygen sensing by ionospheric excitation (ROSIE), Ann. Geophys. , 27, 2183–2189, 2009.

Keiser, B. (1974), Early Development of the Project Sanguine Radiating System, IEEE Trans. Comm., 22(4), 364-371, doi:10.1109/TCOM.1974.1092207.

Kendall, E., R. Marshall, R. T. Parris, A. Bhatt, A. Coster, T. Pedersen, P. Bernhardt, and C. Selcher, Decameter structure in heater□induced airglow at the High frequency Active Auroral Research Program facility, J. Geophys. Res., 115, A08306, doi:10.1029/2009JA015043, 2010.

Kuo, S. P., and M. C. Lee, On the parametric excitation of plasma modes at upper hybrid resonance, Phys. Lett. A , 91 , 444–446, 1982.

Langston, J. and R.C. Moore (2013), High time resolution observations of HF cross-modulation within the D region ionosphere, Geophys. Res. Lett., 40, doi: 10.1002/grl.50391.

Lee, M. C., and S. P. Kuo, Excitation of upper hybrid waves by a thermal parametric instability, J. Plasma Phys. , 30 , 463–478, 1983.

Mahmoudian, A., W. A. Scales, M. J. Kosch, A. Senior, and M. Rietveld, Dusty space plasma diagnosis using temporal behavior of polar mesospheric summer echoes during active modification, Ann. Geophys., 29, 2169–2179, 2011.

Mantas, G. P., Large 6300-°A airglow intensity enhancements observed in ionosphere heating experiments are excited by thermal electrons, J. Geophys. Res., 99 , 8993–9002, 1994.
Mantas, G. P., and H. C. Carlson, Reinterpretation of the 6300-°A airglow enhancements observed in ionosphere heating experiments based on analysis of Platville, Colorado, data, J. Geophys. Res. , 101 , 195–209, 1996.

Merrill, J. (1974), Some Early Historical Aspects of Project Sanguine, IEEE Trans. Comm., 22(4), 359-363, doi:10.1109/TCOM.1974.1092206.

Milikh, G. M., K. Papadopoulos, M. McMarrick, and J. Preston (1999), ELF emission generated by the HAARP HF-heater using varying frequency and polarization, Izvestiya Vysshikh Uchebnykh Zavedenii, Radiofizika, 42, 728-735.

Mjølhus, E., On linear conversion in magnetized plasmas, Radio Sci. , 6 , 1321–1339, 1990.

Mjølhus, E., On the small scale striation effect in ionospheric modification experiments near harmonics of the electron gyro frequency, J. Atmos. Terr. Phys. , 55(6) , 907–918, 1993.

Moore, R. C., U. S. Inan, and T. F. Bell (2006), Observations of amplitude saturation in ELF/VLF wave generation by modulated HF heating of the auroral electrojet, Geophys. Res. Lett., 33, L12106, doi:10.1029/2006GL025934.

Moore, R. C., S. Fujimaru, D. A. Kotovsky, and M. Golkowski (2013), Observations of ionospheric ELF and VLF wave generation by excitation of the thermal cubic nonlinearity, Phys. Rev. Lett., 111 (23), 235007-235011, doi:10.1103/PhysRevLett.111.235007.

Mutiso, C. K., J. M. Hughes, G. G. Sivjee, T. Pedersen, B. Gustavsson, and M. J. Kosch, Previously unreported optical emissions generated during ionospheric heating, Geophys. Res. Lett., 35, L14103 , doi:10.1029/2008GL034,563, 2008.

Nishimura, Y., L. Lyons, S. Zou, V. Angelopoulos, and S. Mende (2010), Substorm triggering by new plasma intrusion: THEMIS all-sky imager observations, J. Geophys. Res., 115, A07222, doi:10.1029/2009JA015166.

Papadopoulos, K., C. Chang, P. Vitello, and A. Drobot (1990), On the efficiency of ionospheric ELF generation, Radio Sci., 25(6), 1311-1320.

Payne, J. A. (2007), Spatial Structure of Very Low Frequency Modulated Ionospheric Currents, Ph.D. thesis, Stanford University, Stanford, California.

Pedersen, T., B. Gustavsson, E. Mishin, E. Kendall, T. Mills, H. C. Carlson, and A. L. Snyder, Creation of artificial ionospheric layers using high-power HF waves, Geophys. Res. Lett. , 37, L02106 , doi:10.1029/2009GL041,895, 2010.

Raghuram, R., R. Smith, and T. Bell (1974), VLF Antarctic antenna: Impedance and efficiency, IEEE Trans. Antennas and Propagation, 22(2), 334-338, doi:10.1109/TAP.1974.1140777.

Rietveld, M. T., E. Turunen, H. Matveinen, N. P. Goncharov, and P. Pollari, Artificial periodic irregularities in the auroral ionosphere, Ann. Geophys. , 14 , 1437–1453, 1996.

Rose, G., B. Grandal, E. Neske, W. Ott, K. Spenner, J. Holtet, K. M°aseide, and J. Trøim, Experimental results from the HERO project: In situ measurements of ionospheric modifications using sounding rockets, J. Geophys. Res. , 90 , 2851, 1985.

Spasojevic, M., H. U. Frey, M. F. Thomsen, S. A. Fuselier, S. P. Gary, B. R. Sandel, and U. S. Inan, The link between a detached subauroral proton arc and a plasmaspheric plume, Geophys. Res. Lett., V. 31, L04803, doi:10.1029/2003GL018389, 2004.

Senior, A., M. T. Rietveld, M. J. Kosch, and W. Singer (2010), Diagnosing radio plasma heating in the polar summer mesosphere using cross modulation: Theory and observations, J. Geophys. Res., 115, A09318, doi:10.1029/2010JA015379.

Swanson, E. R. (1983), Omega, Proc. IEEE, 71, 1140.

Tellegen, B. D. H. (1933), Interaction between radio waves, Nature, 131, 840.

Vas'kov, V. V., and A. V. Gurevich, Resonance instability of small-scale plasma perturbations, Sov. Phys. JETP Engl. Trans. , 46 , 487–494, 1977.

Villasenor, J., A. Y. Wong, B. Song, J. Pau, M. McCarrick, and D. Sentman (1996), Comparison of ELF/VLF generation modes in the ionosphere by the HIPAS heater array, Radio Sci., 31, 211-226.

Wait, J. (1977), Propagation of ELF electromagnetic waves and project sanguine/seafarer, IEEE J. Oceanic Eng., 2(2), 161-172, doi:10.1109/JOE.1977.1145337.

Weisbrod, S., A. J. Ferraro, and H. S. Lee (1964), Investigation of phase interaction as a means of studying the lower ionosphere, J. Geophys. Res., 69(11), 2337–2348, doi:10.1029/JZ069i011p02337.

Woodroffe, J. R., Streltsov, A. V., Vartanyan, A., & Milikh, G. M. (2013). Whistler propagation in ionospheric density ducts: Simulations and DEMETER observations. Journal of Geophysical Research: Space Physics, 118(11), 7011-7018.

Zou, S., et al. (2010), Identification of substorm onset location and preonset sequence using Reimei, THEMIS GBO, PFISR, and Geotail, J. Geophys. Res., 115, A12309, doi:10.1029/2010JA015520.